Open Access

Iraqi Journal for Electrical and Electronic Engineering
Original Article

IJEEE
University of Basrah
College of Engineering

Improvement of Extracted Photovoltaic Power Using Artificial Neural Networks MPPT with Enhanced Flyback Controller

Afrah Abood Abdul Kadhim*, Abdulhasan F. Abdulhasan, Fatimah F. Jaber
Basrah Engineering Technical College, Southern Technical University, Iraq

Correspondance
*Afrah Abood Abdul Kadhim
Basrah Engineering Technical College, Southern Technical University,
Basrah, Iraq
Email: afrah.alasady@stu.edu.iq

Abstract
Due to the nonlinear electrical properties of PV generators, the width and performance of these frames could be enhanced by carrying them to operate at ultimate energy mark tracking. In this study, a versatile maximum power point tracking (MPPT) model using a modified Flyback controller with artificial neural network (ANN) technique as our proposed system. The hybrid Flyback/ANN controller is based on teaching and training a neural network, where the dataset is utilized to adjust the levitation converter which is taken care of by a stand-alone photovoltaic generator (PVG) with a Flyback controller. It is assumed that the results will be obtained by the ANN-MPPT system with the Flyback controller which provides low motions and shows a great implementation around the maximum power point compared to the PVG used with traditional MPPT algorithms such as Perturbation and Observation (P & O).

Keywords
Maximum Power Point Tracking (MPPT), PV Generators, Photovoltaic Cells Generator (PVG), Flyback Controller, Artificial Neural Network (ANN) Algorithm.

I. INTRODUCTION

In recent years, the integration of sustainable energy sources has become prevalent across various industrial and domestic applications. These sources, often referred to as clean, renewable resources, offer significant environmental benefits compared to fossil fuels, which have long been associated with detrimental impacts on the environment. Among these sustainable sources, solar energy stands out as a primary choice due to its abundant availability and minimal environmental footprint [1–5]. However, despite the advantages of solar photovoltaic (PV) systems, their efficiency is heavily influenced by external factors such as temperature and solar radiation intensity. Variations in these parameters can significantly affect the power output of PV systems, making it essential to employ robust MPPT techniques to ensure optimal performance and efficiency [6–11].

The latest articles too investigation papers covering the title of the work are recorded as under: There has been a lot of investigation on vision-based road way affirmation. Various methodologies for straight with twisted way disclosure have been suggested through the most ongoing decayed. The PV power overflow produces potential vacillation in the low-voltage conveyance grid. All together to dispose of this issue, another PID control plot for the ANFIS-relied PV interface inverter with ANFIS-relied monitored power limit the board framework for PV framework association is suggested in [12]. In addition to suggesting the fuzzy rationale-based control scheme for the battery energy storage system (BESS), [13] illustrated the reasonableness of the fuzzy controller for controlling the DC transport potential. In [14], using a fuzzy interface system (FIS), a scheme with sustainable power supplies is presented along with a load unit for the administration of the power

stockpiling plan. The suggested structure was contrasted with a standard-relied control technique, which demonstrated that the suggested FIS could diminish fluctuation by growing the energy stockpiling system (ESS's) existence design. A structure prescient control procedure, relying on climate gauges, is suggested to decrease the power interest as well as augmentation the use of sustainable power hotspots for driving the board in local smaller than usual grids [15]. The arranged MPC control system relies on addressing a restricted ideal control issue for a specific period outline skyline. Such suggested framework was contrasted as well against the ordinary rule-relied control rationale. An enhancement in house solace constraints with a typical 14.5 % decrease in the use of essential fossil power is taken note of. The high entry of renewables changed the movement of ideal models of power frameworks. To adapt to these changes, the power of the executive's frameworks has become major taking everything into account [16–20]. Control as well as trading-based power in the executive's framework is suggested for the micro-grid framework comprising of wind, and PV with battery [21]. The suggested energy management system (EMS) is accessible regardless of mains. Such a framework may be synchronized against various sources to shave load power throughout the operation time at whatever point it is the greatest burden. For instance, depending on the system, else air is utilized as the essential energy supply, and PV is consolidated to fabricate the unwavering nature of the framework in various climate circumstances. The battery unit is employed as a power stockpiling framework throughout reinforcement power when the wealth of power or potential interest is in [22]. To oversee power supplies disseminated along small-size power focuses, a self-restoring computation that oversees ideal power streams is suggested to accomplish the least power costs dependent upon the power, charges as very much expected load interest along each supply in [23]. MPC with creation, use, and battery with esteem limitations is expected for a grid-associated framework comprising wind, and PV with battery [24]. Besides here survey, it was normal to select the suitable supply as well as produce the ideal ability to the interest view. Operative-arranged cerebrum network-relied control framework is suggested for MPPT. To decrease the energy top along the grid, fuzzy rationale-relied EMS is arranged. A fuzzy rationale-relied EMS is suggested to restrict vacillations with grid-tied Micro-grid pinnacle energies [25]. The traditional fuzzy genetic estimation procedure is suggested in articles [26]. Double various GAs are employed. The essential GA sets the microgrid's energy organizing as well as fuzzy principles, and the second GA groups the fuzzy investment capacities. fuzzy master frameworks are likewise utilized in battery power the board. Power the board is suggested using a multi-objective particle swarm optimization procedure for

a grid-associated micro-grid comprising of power breeze PV-FC battery in [27]. It is planned to accomplish the greatest power age along each supply and to lessen the functioning expense of the microgrid. A cross-breed estimation is made utilizing PSO with brilliant wolf optimization (GWO) as well as day-ahead booking settled power the board technique is suggested in [28]. A half as well power the board computation is suggested by modifying the standard base of the fuzzy determination framework against the hierarchical genetic algorithm (HGA) in [29]. The fuzzy HGA computation seems to be ideal over the traditional fuzzy GA procedure, utilizing just 46.9% of the guidelines inside the standard base. By getting a less troublesome sensitive rationale controller, the entire control framework can be executed progressively on minimal expense implanted electronic gadgets. The grid-associated micro-grid comprised of wind, PV, strong oxide force circuit (SOFC) supplies, and BESS with two practically identical DC with AC loads [30]. Fuzzy rationale-based power for the executives is suggested for a half-with-half framework comprising of PV-FC battery [28–30]. Continuous with long-haul anticipated data is used at the power age also usage. In the arranged framework, multiport converters with alluring transport are utilized to lessen potential change phases. A nonlinear MPC method is suggested in [30]. A fake neural network was employed for resistive box assessment. Battery condition of charge (SOC) control with burden wanting to guarantee potential security. Grid associated suggested an MPC-relied EMS in [28–30]. By growing the utilization of wind energy with battery, the energy got along the grid as well the energy charge is diminished. To restrict the expense of power along the grid, utilizing Gaussian interaction (GP) assessment of what's straightaway, MPC power the board is suggested in [29, 30]. Against the GP, PV yield power with burden need power is assessed. An improvement-based MPC strategy is employed.

This paper aims to explore and propose novel approaches for enhancing the performance of MPPT systems using two controllers on the boost converter PV cells framework and investigated utilizing a hybrid flyback controller with artificial neural network controllers. The proposed methods aim to improve the accuracy and adaptability of MPPT systems across varying environmental conditions, ultimately contributing to the stability and efficiency of solar PV systems.

II. METHODOLOGY

In this part, the basic theoretical concepts of photovoltaic array control using artificial neural networks (ANNs) are addressed through mathematical equations and illustrative diagrams. The basic principles of photovoltaic operation will be discussed in detail with examples of practical implementation and illustrations. Also, common types of DC-to-DC

boost controllers will be explained supported by equivalent operating relationships and characteristic diagrams. Finally, the structure of the ANN controller will be analyzed through complete scientific treatment and comprehensive clarification.

A. Photo Voltaic Cells Power Supply

The solar panel includes a homogeneous mass of solar-absorbing glass sheets, succeeded by solar cells, which are a photovoltaic array that operates to implement a group of photovoltaic (PV) units to convert the sun's rays into a continuous electric current. The array consists of a series of units attached in parallel, and each series consists of units linked in an integral series. Such block permits the modelling of pre-selected PV modules with the System Advisor Model (2018), National Renewable Energy Laboratory (NREL) against the PV modules we select. The equivalent circuit of the PV cell is shown in Fig. 1. However, the characteristic of the solar cell is illustrated in Fig.2,
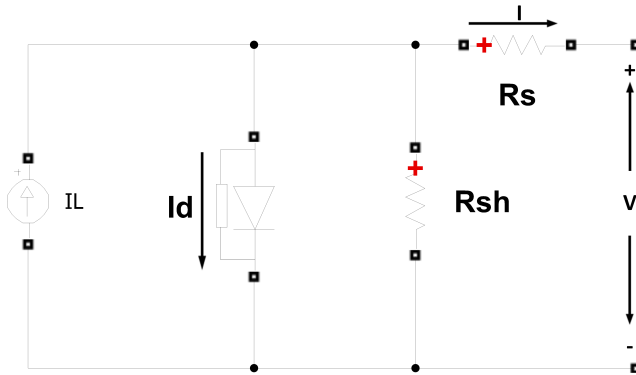

Fig. 1. The PV cell unit equivalent circuit [4–6].

The I-V diode characteristics are shaped for a specific module by the below equations:

$$I_d = I_0 \left(e^{\frac{V_d}{V_T}} - 1 \right) \qquad (1)$$

$$V_T = \frac{KT}{q} \times nl \times N_{cell} \qquad (2)$$

Where,I_d is the current was routed through a one-of-a-kind diode,V_d is the diode's voltage through it(V),I_0 is the diode's reverse saturation current, VT is the terminal voltage, K is The constant of Boltzmann $(1.381 * 10^{-23} J/K)$,T is the temperature of the cell (K), q is the charge of electrons $(1.602 * 10^{-19} C)$, nl is the ideality factor for the diode, and N cell is the number of cell in the diode structure.

These PV cells will be the essential power supply of the system that will produce the network against the needed power. The illustration of such a unit is as follows: PV array implemented over a series of PV modules is parallel attached.
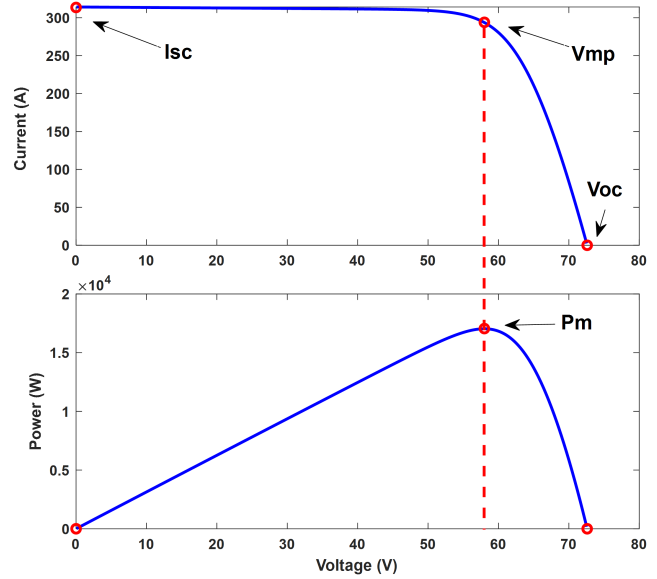

Fig. 2. PV cell power and current characteristics [4–6].

Every series consists of units attached in series. Such a unit allows the modelling of a diversity of pre-selected PV modules possible along the NREL System Advisor Model against a user-defined PV module. Input 1 = solar irradiance in W/m2 and input 2 = cell heat in degrees Celsius. The circuit diagram of the PV array unit implemented using MatLab2020b Simulink structure is presented in Fig. 3.
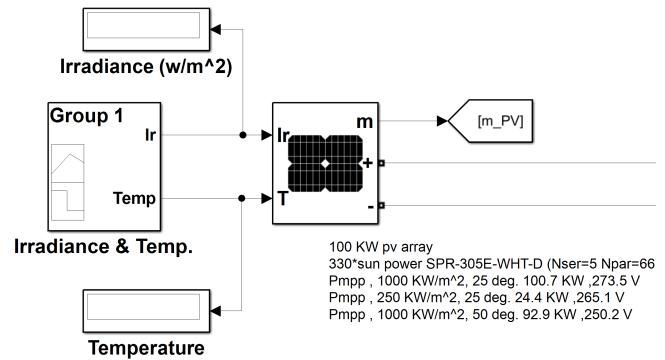

Fig. 3. The photovoltaic module.

The solar irradiance intensity, ir, and heat temperature, T map signal builder unit is displayed in Fig. 4.

B. DC to AC Power Inverter System

Inverters might be considered as a demonstration of a classy of devices named power electronics that control the electrical power flow. In essence, the inverter performs the DC-to-AC conversion by rapidly switching the DC input's orientation.
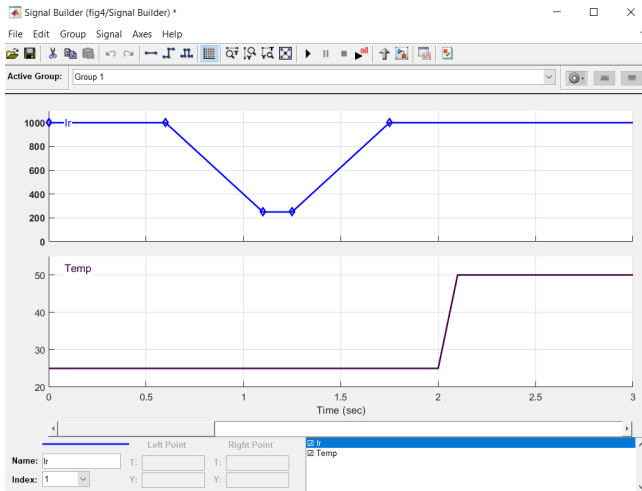
Fig. 4. The solar irradiance intensity and heat temperature of PV module [4–6].

The AC output waveform emerges from the DC input as a result. A common DC-to-AC inverter is displayed in Fig.5. Concerning the switching operation, there are various techniques and approaches possible in publications to obtain the suited switching operation. The switching process is the ultimate important of the performing converted AC voltage signal quality.
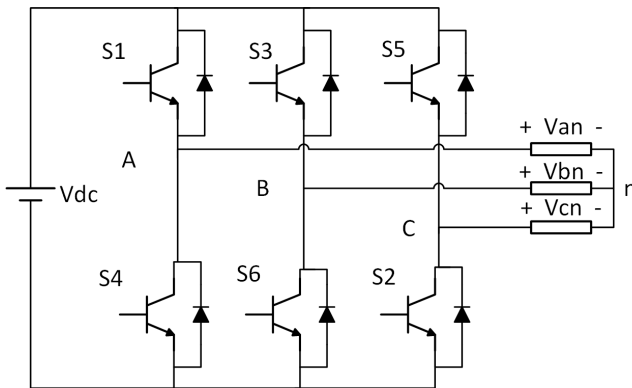

Fig. 5. A typical DC-to-AC inverter circuit diagram [15].

Usually, DC to AC inverters are efficiently designed utilizing Neutral Point Clamped (NPC) inverters. Such type of inverters is a group of multi-level transducers that feature the use of stabilization diodes to ensure proper voltage sharing across the power switches. NPC adapters or inverters circuit diagram is presented in Fig. 6.
Furthermore, the NPC inverter signals produced by the controlling circuits have been illustrated in Fig.7. The selection of the inverter switches controller is a very necessary aspect in determining the DC to AC signal transformation quality.
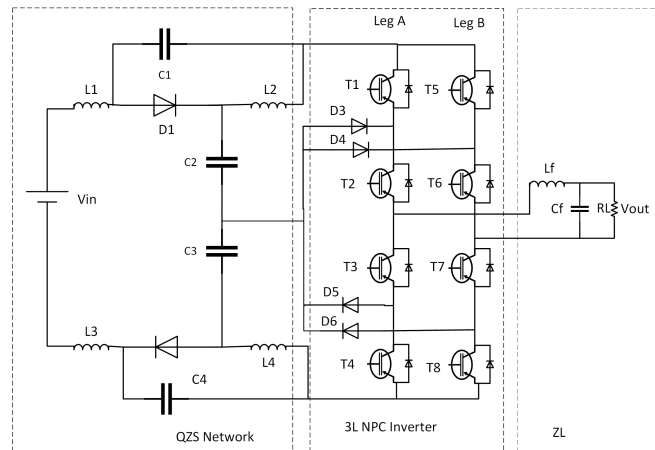

Fig. 6. The NPC inverters circuit diagram [14–18].

The obtained AC signal will suffer from total harmonic distortion (THD) due to the high switching pulses and the deficiency of the current control circuit and the interaction with the harmonic voltage background of the grid at the point of connection. The advanced studies are interesting in varying the widths of the switching time such that resulting in varying width pulses which minimize the THD.

C. The Boost DC Voltage Converter Circuit

Boost converters are defined as planned to increase an alternating solar panel voltage to a larger consistent DC voltage. It applies voltage feedback to maintain the resulting voltage consistent. Such a section is very essential to obtain the maximization of the DC supply voltage and sustain constant ultimate available DC power to the scheme. The circuit diagram of the Boost DC voltage Converter unit implemented along the MATLAB 2021b Simulink model is illustrated in Fig.8. The boost converter connects the PV cells with the DC to AC inverter and acts to increase the DC voltage to its maximal values and prevent or reduce their fluctuations to achieve the best obtained DC amount for AC conversion preparations. The boost converter might be controlled with various techniques and controllers to obtain the maximum point power tracking (MPPT) which ensures the best DC voltage performance from the PV arrays. The MPPT concept with the common applied controllers will be discussed in the following sections.
Usually, the MPPT controller is utilized to ensure the operation of the PV array at the maximum power point power even with the variation of solar irradiance values. Fig.9 displays the MPPT performance for PV panels [12–18].
Several types of MPPT controllers are available that act to maximize the DC voltage from PV cells and enhance the DC voltage fluctuations also the overall performance. In this project, three types of MPPT controllers will be illustrated
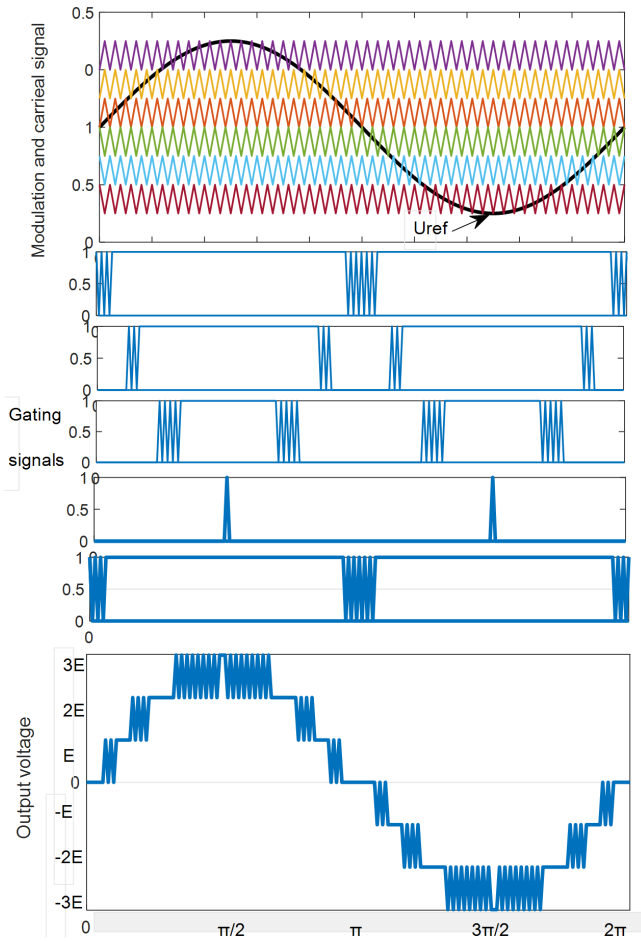
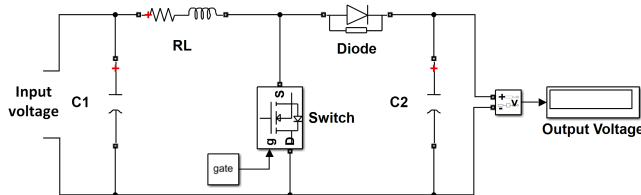Fig. 7. NPC inverter switching pulse signals [14–18].

Fig. 8. The boost converter circuit, implemented with MatLab2021b Simulink toolbox [10–15].

which are listed below points: 1)Perturb and Observe (P & O) algorithm,
2)Voltage source converter (VSC) controller, and
3)Artificial neural networks (ANN) controllers.

1) Perturb and Observe (P & O) Algorithm

The algorithm is based on continuous operation of observation and perturbation until the operation point converges to the
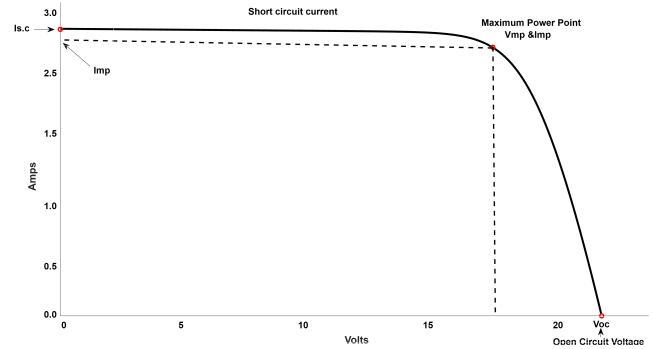

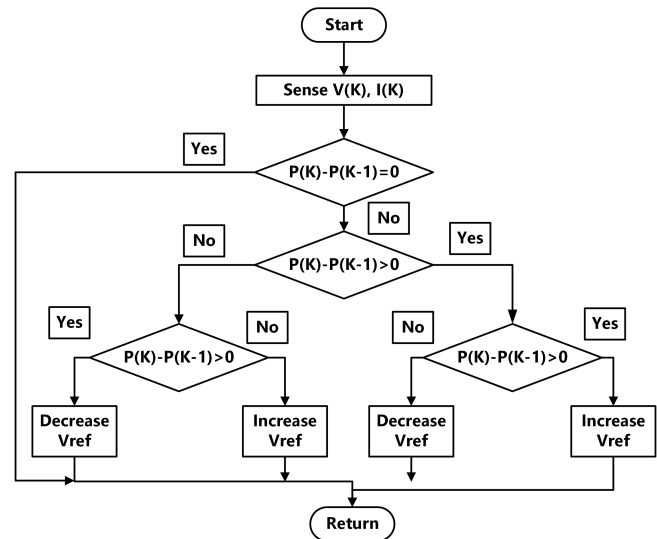Fig. 9. MPPT performance for PV panels [12–18].

Fig. 10. Flow chart of P & O algorithm.

maximum point by calculating the output power and adjust a photovoltaic system by sampling both the photovoltaic current and voltage. The tracker works by periodically increasing or decreasing the voltage of the solar array. Fig. 10 shows the flow chart of the P & O algorithm. So, a small voltage perturbation changes the solar PV power if the power is positive alteration, voltage perturbation is continued in the same way otherwise if the change of power is negative, it refers that the maximum point is far away and the perturbation should be decreased to reach the MPP. As a result, the DC chopper's duty cycle is adjusted, and the procedure is carried out again until the MPP has been reached.

2) Voltage Source Converter (VSC) Controller

Self-switching transformers called voltage-selected controllers (VSCs) are used to connect high-voltage alternative current (HVAC), high-voltage direct current (HVDC), and low-voltage alternative current systems using IGBTs and other electronic devices. VSCs can switch on themselves, producing AC volt-

age without the need for an AC system. Independent control of active energy against reactive energy, AC voltage compensation, and a suitable installation size are among the advantages of VSC [16–22]. Fig. 11 depicts the phase-locked loop (PLL) circuit diagram for the VSC controller. In the phase-locked
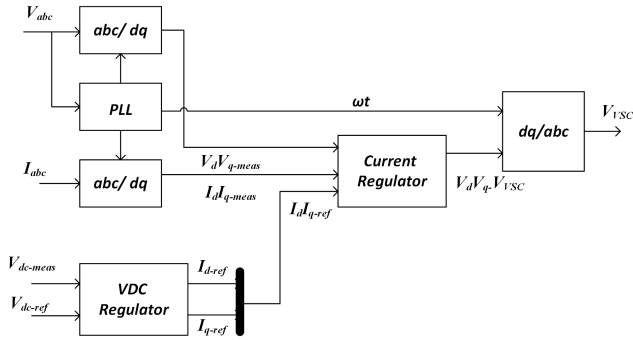

Fig. 11. The VCS using PLL controllers circuit diagram for MPPT [14–18].

loop, PLL converts, vabc to vdq, and dynamically controls the rotational velocity of the dq-frame to maintain vq = 0 [5]. The equation of the PLL operation might be written as:

$$v(t) = V_p \cdot e^{(\omega t + \theta_0)} \tag{3}$$

Also,

$$v_d = V_p \cdot \cos\left(\omega t + \theta_0 - \theta(t)\right) \tag{4}$$

$$v_q = V_p \cdot \sin\left(\omega t + \theta_0 - \theta(t)\right) \tag{5}$$

By selecting $\theta(t) = \omega t + \theta_0$ the required outcome of having $vq = 0$ is achieved. There are many various PLL techniques possible, yet synchronous reference frame phase-locked loop, SRF-PLL is the typical structure in three-phase PLL implementations [18–20]. This was rather the part utilized in this section. Fig. 12 presents the SRF-PLL block diagram. The input waveform vq is fed toward the PI controller resulting the angular frequency deviation $\Delta\omega.\omega = 2\pi f$ is next summed to this that is integrated into θ_0 at last. As it might be noticed in Fig. 13, it might be expressed by:

$$\theta = \int \omega_g dt = \omega t + \int \Delta\omega_g dt \tag{6}$$

The voltage-selected controller (VSC), might be implemented also using a pulse width modulation (PWM) strategy as shown in Fig. 13.
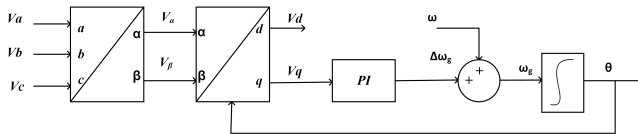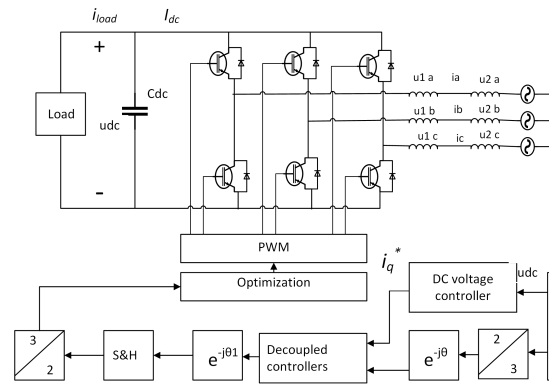

Fig. 12. Block diagram of SRF-PLL [14–18].

Fig. 13. The VCS using PWM controllers circuit diagram for MPPT [14–18].
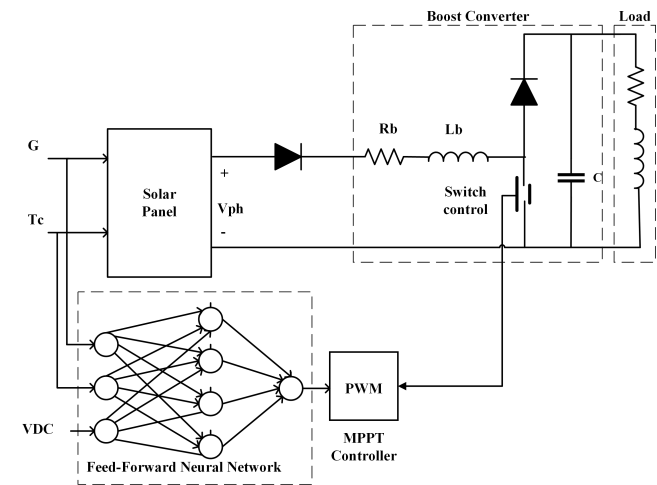

Fig. 14. Common ANN controller for PV power system [15–19].

3) *Artificial Neural Networks (ANN) Controllers*

Artificial neural network controllers are powerful data-driven modelling equipment that is broadly utilized in the dynamic modelling as well as quantification of nonlinear systems, because of their global approximation abilities with their flexible structure which permits capturing complicated nonlinear performances. The ANNs are biologically inspired computer software analyzed to simulate the approach that the human brain processes data. ANNs collect their knowledge by discovering patterns and relationships in data and learn (or are trained) along practice, not along automation. Fig. 14 presents a common ANN controller for PV power systems. Thus, ANN is part of the improved monitor techniques. It is utilized for monitoring the system attached to the three-phase photovoltaic grid with such ANNs. They have been successfully applied in the advancement, of associative memories, pattern recognition, and numerous other fields [16–20]. ANN is utilized in

such models due to that it has several benefits as NN Artificial kinds of artificial intelligence (AI) is part of the enhanced monitor categories also, no force is required for model description, NN contains an input layer, output layer, and hidden layers number as displayed in Fig. 15. The entered layer is based on controlling the current that includes of two axes (d axis and q axis). Also, the outcome layer is expressed by the monitor waveform axis. The hidden layer in the ANN archi-
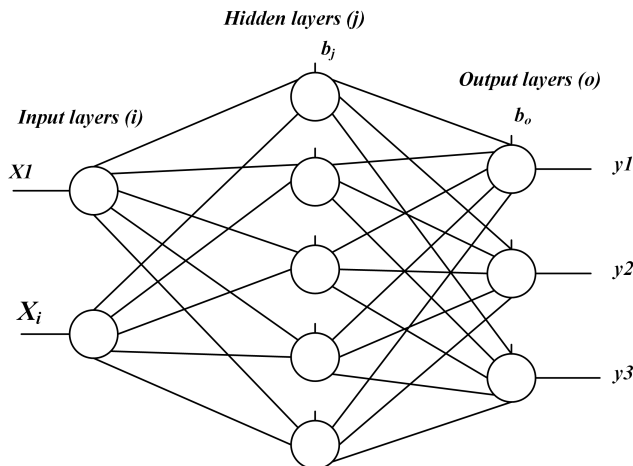

Fig. 15. Schematic diagram of Neural network internal model [16–20].

tecture includes many neurons organized into layers. Each neuron in each layer is fully connected to each part of the neuron. Fig. 16 shows a block of the developed feed-forward neural network. The inner layer consists of 10 hidden layers and one output layer. The information layer of this network is the current error of the reference frame in the axis component [16–22]. Since ANN controllers have been nominated to be chosen as the proposed model in this study, the details of the types and categories of ANN models and activation functions will be discussed in chapter three with analytical equations and illustrative diagrams. In this suggestion, we propose an effective controller for adjusting the photovoltaic micro-grid power system with the help of the ANN technique to solve the issue of floating power and improve the efficiency of the system as a whole. The suggested model ought to be
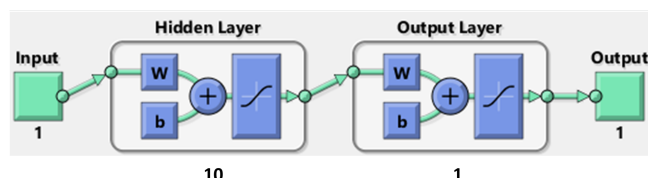

Fig. 16. Block diagram of the designed neural network internal structure [16–21].

capable of cancelling the losses and disadvantages caused by LC filters as well as other control technique limitations. The necessary programming has been decided to utilize the proposed procedure transfers after using the MatLab2020 recreation program. This product allows the creators with proficient devices to recreate the issue likewise to introduce the fundamental assessment bundles. MatLab2020 recreation program comprises a strong fantastic implicit customized capabilities that have been used in our proposed re-enactment strategy. Fig. 17 shows a screen capture of the underlying Enhancement devices given by MatLab2020b (Applications) utility which will be utilized in the suggested technique.
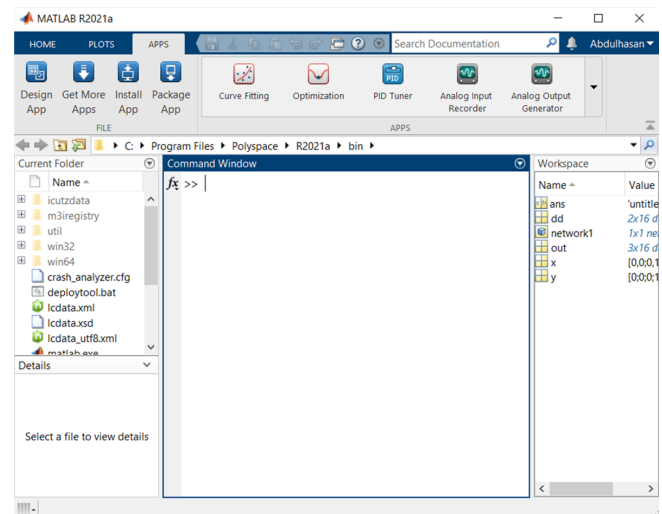

Fig. 17. Matlab 2021a application program utilized in the project.

D. The Flyback Converters

Concerning the flyback converters which are flexible power electronic devices utilized in applications like medical devices and versatile PCs. Otherwise called isolated buck-boost converters, these converters are basic circuits that can control the framework yield voltage (VOUT) while decreasing electromagnetic interference (EMI). A flyback transformer is an inductor coupled to a gapped core. During each cycle, when an information voltage is employed in the primary loop, power is stored in the core gap. It is then transferred to the secondary loop to supply capacity to the load. Fig. 18 demonstrates a circuit diagram of a flyback converter [18–22]. The internal structure of flyback transformers is of the similar essential components as utmost similar interchanging transformer configurations; however, the distinguishing component of the flyback transformer is its dual inductor that insulates the transformer's contribution along its result. The name "flyback" is due to the unexpected stopping/stopping, turning

on/off of a MOSFET switch, where the waveform resembles a sudden reversal of current. The result is regulated by setting the on/off pattern of the primary side switch. The flyback converter has dual wave half-instants: tON and tOFF, which are called later (also restricted to) the alternating MOSFET phases. Through tON, the MOSFET is in the on state, and current streams along the contribution along the initial inductor linearly charge the coupled inductor. Through tOFF, the MOSFET is in the off state, with the coupled inductor starting to demagnetize along the diode. The current along the inductor charges the load resulting capacitor with power. There are many important plan choices and trade-offs engaged in planning a flyback converter. The accompanying segments will go along every move toward the planning cycle for a basic flyback converter. Fig. 19 displays the planned stream of the flyback converter [18–22].

The flyback capability served navigation and timing game purposes in the next 100 years. It was the principal watch complication intended to record various instant periods, for example, calculating the time taken to travel amidst waypoints, compute fuel consumption, or achieve coordinated manipulators.

The suggested model simulation diagram has been presented in Fig. 20 to illustrate the methodology of its operation.

The above diagram displays the simulated model consisting of three main units, the photo voltaic cells, the boost controller, and the hybrid flyback with ANN controller unit. Concerning the boost converter unit, the provided voltage and current signals from the photocells unit will be analyzed and converted to be enhanced. The construction of the simulated boost converter unit will be shown in Fig. 21.

A DC-to-DC power converter known as a boost converter or step-up converter raises the voltage while decreasing the amount of current flowing along its entrance (source) to its outcome (weight). It is a kind of switched-mode power supply (SMPS) that consists of at least two semiconductors—a diode and a transistor—and a partially single power-saving component: either an inductor a capacitor, or a combination of each. To lessen potential ripple, capacitor-based filters are typically added to the converter's supply-side filter and load-side filter, respectively. Refrigerators, batteries, solar panels, DC generators, or any other DC source that works can power the boost
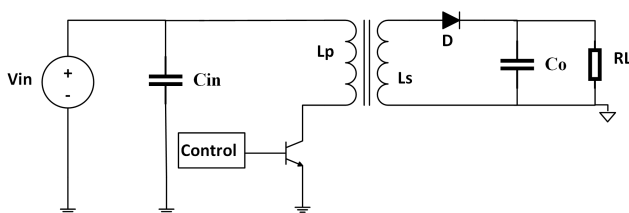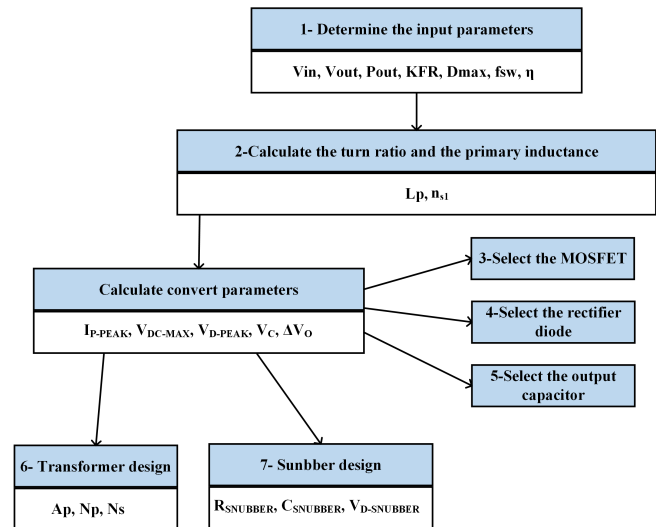

Fig. 19. the plan stream Flyback converter [18–22].
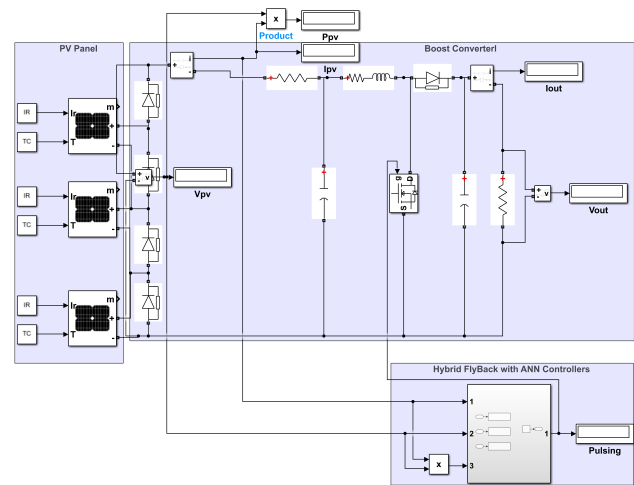
Fig. 20. The suggested simulated scheme block diagram.

Fig. 18. Circuit diagram of a flyback converter [18–22].

converter. The process of converting one DC voltage into another DC voltage is known as DC-to-DC conversion. A boost converter is a DC-to-DC converter whose output voltage is higher than its source voltage. A boost converter is sometimes referred to as a step-up converter because it "steps up" the source voltage. Due to the need to conserve power (display style P=VI) and P=VI), the output current is lower than the source current. The hybrid flyback with ANN controller unit is the essential unit in the simulated model, which is responsible for the optimum or maximum power tracking that might be obtained from the model. It consists of two main controllers, the flyback controller, and the artificial neural network (ANN) controller. Fig. 22 presents the implementation model of this hybrid controller.
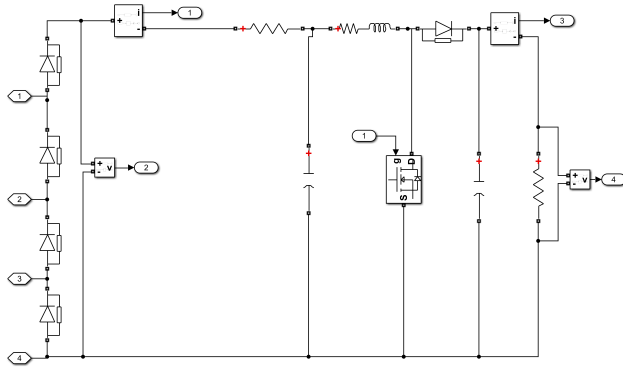
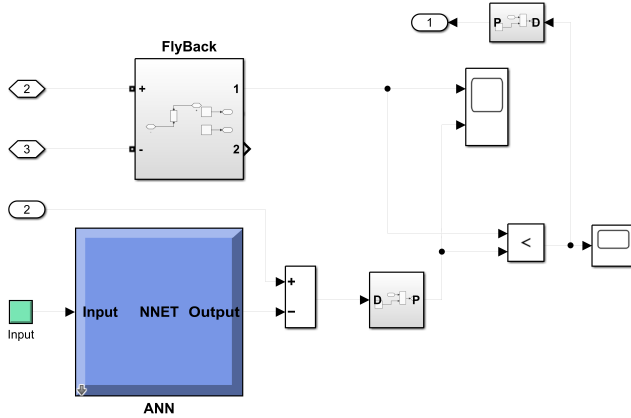Fig. 21. The construction of the simulated boost converter unit.

Fig. 22. The implementation model of the hybrid controlling technique.

Fig. 23. The construction of the Flyback controller technique.

(a)

(b)

Fig. 24. The ANN controller construction, (a) ANN internal layers, (b) ANN layer construction.

Every controller will act on the differential change in PV voltage and current to produce the differential change in overall obtained power. This differential change will be maximized until achieving the maximum power at the output of the model. Fig. 23, and Fig. 24 illustrate the construction of the P & O controller and the ANN controller respectively.

Such structure introduces a converted crossover greatest power point to ensure that photovoltaic (PV) displays under partial shade (PSC) conditions can always produce maximum power quickly and effectively. The strategy that comes next is called MPPT, and it involves applying a specialized neural network (ANN) to the modified perturbation and monitoring (the flyback controller unit). Instead of using expensive luminous intensity sensors straight away, the luminous intensity is turned on for each PV cluster unit, and the given points can be checked by using the cheapest voltage and current sensors. The ANN anticipates the optimal voltage areas for the Global Maximum Power Point (GMPP) by utilizing the backhanded light i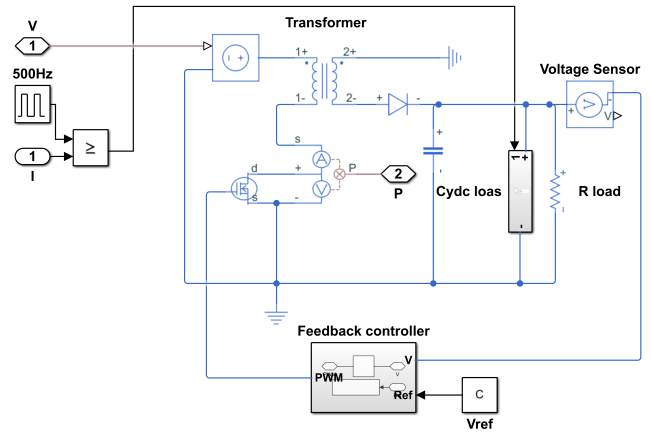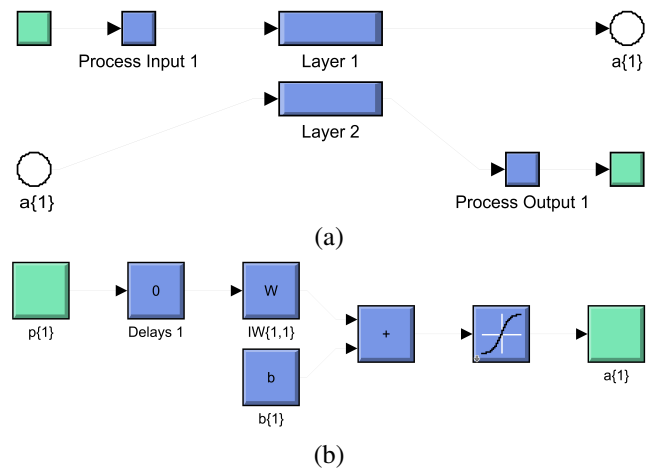ntensity. The combination of the flyback controller with the ANN controller will provide better tracking to the overall power since part of the very small differential change in the PV voltages and current that might not be sensed by the flyback controller will be detected by the ANN algorithm controller system.

III. RESULTS AND DISCUSSION

The simulated structure of the suggested PV system inverter characteristics improvement using the ANN controlling technique system has been implemented using the MatLab2020b Simulink toolbox. The simulation structure of the suggested model has been illustrated in Figs. 20-24.The design parameters utilized to set the implement the simulation scheme are summarized in Table I.

TABLE I.
THE DESIGN PARAMETERS UTILIZED TO IMPLEMENT THE SIMULATION MODEL

Design Components	$Rs(\Omega)$	$C1(F)$	$R1(\Omega)$	$L1(H)$	$C2(F)$	$Rp(\Omega)$
Values	0.2	200e-6	10	2e-3	200e-6	1000

A. Achieved Results

The generated PV cell's voltages, currents, and power signals are presented in Fig. 25. It is clear from the obtained results that the values of the PV voltage and current are unstable and the resulting PV power reaches unstapled values and fluctuates below the maximum designed amount. On the other hand, the values of supplied current also fluctuate below 20 A, while the voltage is reaching to more than 1000 V because the cells are connected in series.

Now, the resulting signals along the ANN controller are displayed in Fig. 26. Now, the resulting signals along the ANN
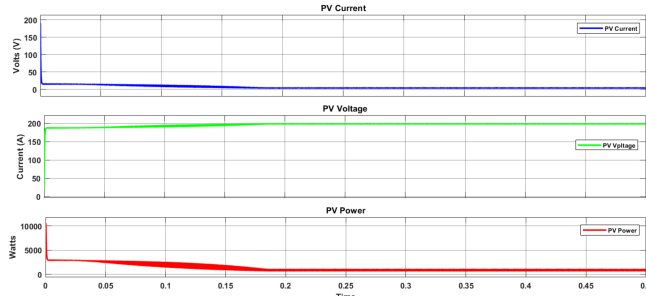

Fig. 25. The generated PV cell's voltages, currents, and power signals.

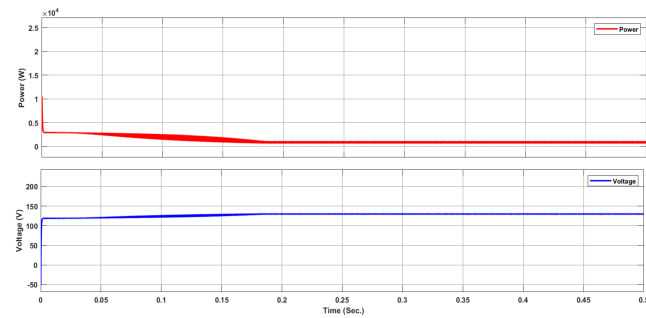controller are displayed in Fig. 26. The upper red-coloured

Fig. 26. The resulting signals from the ANN controller.

signal is the controlled power signal as the result of the ANN controller, and the lower blue-colored signal is the resulting controlled voltage signal. Next, the output waves from the flyback controller compared with the ANN controller are illustrated in Fig. 27.

The upper blue colored signal is the flyback controller signal before comparison with saw tooth pulses and represents the
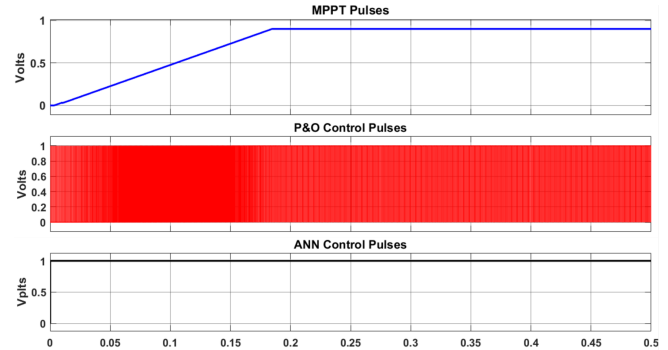

Fig. 27. The output signals from the P & O controller compared with the ANN controller.

variations of the differential changes between voltage and current of the PV cells after forcing the circuit to produce the maximum power. The second red-colored signal is the output pulses obtained from the flyback controller after comparing the differential varied blue signal with the saw tooth pulses to get the controlling pulses to the boost converter. At last, the third black-colored signal is the output pulse from the pulse width modulator (PWM) after the ANN controller. This signal also represents the observation of the differential alternation in the PV voltage and currents entered into the ANN algorithm, in which the maximum power will be achieved. These controlling pulses will be applied to the boost converter to optimize the entered PV cell's DC voltage and current signals and achieve maximum power tracking value MMPT as presented in Fig. 28.
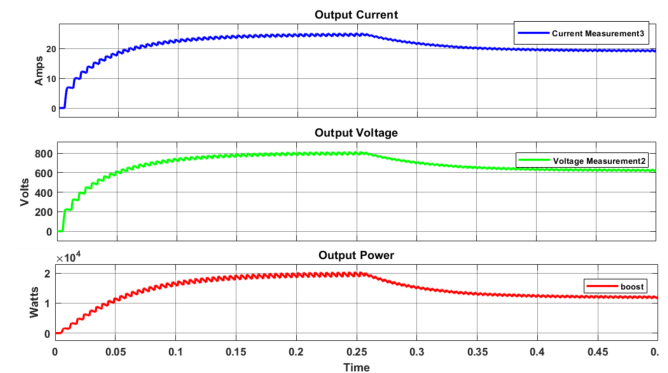

Fig. 28. Resulting maximum power tracking point MMPT signals using hybrid flyback-ANN controller.

It is obvious from Fig. 28 that, the hybrid controller operates to obtain the best MMPT results as the power reaches to more than 20 KW as presented with the red-colored curve. This has been achieved by tracking the maximum current and voltage of the PV cells utilized in the simulation so that, the final current reaches to 22 A as shown in the blue-colored curve, with a final overall voltage of 1150 V.

B. Results Comparison & Discussions

By reviewing the results achieved from implementing the suggested system we found that the use of smart ANN algorithms for PV-MPPT with Flyback controllers will assist in providing proper and appropriate MPPT results with high DC to ac conversion. To complete the idea of research and thesis, we can compare the results obtained from the simulation of the proposed technology with the results of the same system, but using the traditional P & O type controller. Fig. 29 shows the design structure of the solar cell system simulation model with a boost converter using the P & O strategy.
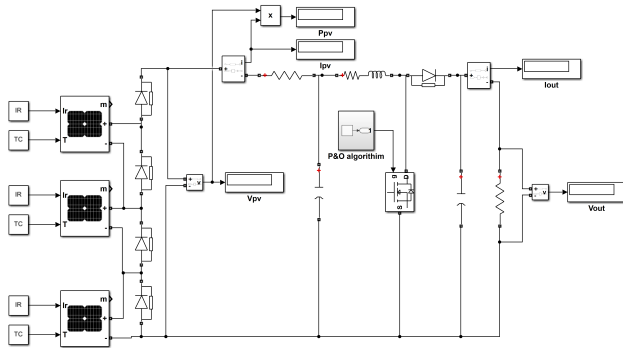

Fig. 29. The design structure of the solar cell system simulation model with a boost converter using the P & O technique.

Using the similar design parameters implemented with the hybrid model illustrated in Table I, the yielding MPPT signals are displayed in Fig.30.
As it is clear from the obtained results of the simulated model using a typical P & O controller, the final tracking power is only 3000 W which is much less than that obtained by the hybrid model. Also, the achieved final voltage and current result with lower values of 400 V and 9 A. Furthermore, the same PV boost converter simulation model is implemented but with the ANN control technique without applying the P & O strategy. Applying the similar design parameters implemented with the hybrid model illustrated in Table II, the resulting MMPT signals are displayed in Fig. 31.
As it is observed from the achieved results of the simulated model utilizing a typical ANN controller, the final tracking power is only 1000 W which is still much less than that ob-
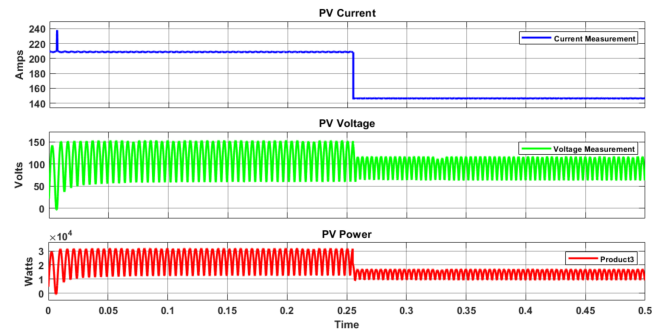

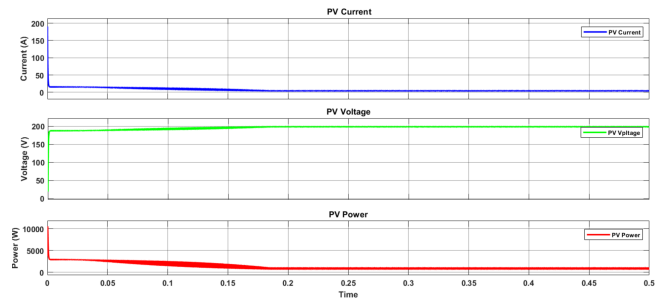Fig. 30. Resulting maximum power tracking point MMPT signals using P& O.

Fig. 31. Resulting maximum power tracking point MMPT signals using ANN controller.

tained by the hybrid model. Also, the achieved final voltage and current result in lower values of 250 V and 4 A. By such results, the conclusion is clear that the simulation model with the hybrid flyback-ANN controller has better MMPT performance by 4 times that obtained using only P & O control. Table II summarizes the comparison of the obtained results for the three techniques.
Moreover, the results of the model we propose in this paper were compared with those presented by recent scientific articles and studies. Table III shows a brief comparison of our proposed model with those provided by recent published studies.

IV. Conclusions

In this paper, the impacts of blending two controllers on the boost converter PV cells framework have been examined and investigated utilizing a hybrid flyback controller with artificial neural network controllers. The ideal voltage at which the loads get the most power with the least misfortunes is known as the maximum power point tracking (MPPT). Three photo voltaic (PV) penal cells have been used as constant DC power sources to give a partially shaded direct current to the framework. The planned PV cells model has been simulated and examined with three kinds of boost controllers. The

TABLE II.

COMPARISON SUMMARY OF THE OBTAINED RESULTS FOR THE 3 TECHNIQUES

Control Technique	D.C. Current I (Ampere)	D.C. Voltage V (Volts)	MMPT P (Watt)
ANN	4	250	1000
P& O	10	500	5000
Hybrid	20	1250	25000

TABLE III.

A COMPARISON SUMMARY OF OUR SUGGESTED MODEL WITH THOSE PRESENTED BY MODERN PUBLISHED STUDIES

Reference	Strategy	Implementation	Limitations
In 2019, Easley, M., et. al., [5]	Auto-Tuned Model Boundaries in Prescient Control of Force Gadgets Converters	Alterations of limited set model prescient control are made for different applications, showing the way that repetitive problems of limited set MPC can be addressed. Issues of uncertain expense capability plans and, for certain applications, illogical computational weight are tended to. A variety of the limited set MPC is proposed which eliminates vagueness in the plan period of the limited set MPC. Utilizing progressive model prescient control, arrangements that empower real-time model arrangement, issue lenient activity, and situational consciousness of the transformer are introduced. These enhancements in prescient control can guarantee that the upcoming array brilliant inverters are quick, mindful, and solid.	The tracking performance required for each target is determined during design. Assuming multiple objectives, the designer must rank each objective and apply its associated cost tolerance (or acceptable error) to the objectives. Also, complicated scheme with large computations & increased temperature.
In 2021, Khalilzadeh, M., et., al., [6],	Boundary Free Prescient Control of IPM Engine Drives with Direct Determination of Ideal Inverter Voltage Vectors.	The time subordinates of the armature current (slants) are communicated as elements of the stage points of the inverter's key voltage vectors. The slants are then anticipated freely of the engine boundaries and are utilized in choosing the ideal inverter voltage vectors. Furthermore, a strategy is utilized to keep away from time-consuming assessments of the expense capability to decide the ideal inverter voltage vector. Through this technique, reference current inclines are utilized to choose the ideal direct voltage vector. Thus, the control execution under parametric vulnerabilities is improved and the control code execution time is abbreviated contrasted and with the conventional prescient strategy. The adequacy of the proposed technique and its prevalence over the conventional strategy and the late presented prescient current control strategy is affirmed by reproduction and exploratory outcomes.	Complicated Structure with high cost. Also huge number of computations to select the optimum inverter voltage vectors.
Our Suggested Model	PV system inverter Characteristics Improvement using Flyback/ANN Controlling technique	By studying here, we present a superior way to eliminate the power of MPC to guide variant/fault combinations with a truly executable bounds evaluation. Moreover, we extend the proposed method to better working conditions through a new artificial neural network strategy. New predictable evaluation accuracy results of over 96 % have been achieved in total harmonic distortions (THD) of normal MPC for apparent properties.	Little delayed testing against commutations with acceptable complexity and medium cost.

simulation results show that the hybrid combination of the Flyback-ANN regulator provides the best maximum power point tracking (MPPT) among the two different controllers. The proposed model creates an MPPT power of 25 KW which is on numerous occasions better compared to both the P & O method and the ANN regulator for each individual

CONFLICT OF INTEREST

The authors have declared no conflict of interest.

REFERENCES

[1] J. Matevosyan, B. Badrzadeh, T. Prevost, E. Quitmann, D. Ramasubramanian, H. Urdal, S. Achilles, J. Mac-Dowell, S. Huang, and V. Vital, "Grid-forming inverters: Are they the key for high renewable penetration?," *IEEE Power Energy Mag.*, vol. 17, no. 6, pp. 89–98, 2019.

[2] O. Babayomi, Z. Li, and Z. Zhang, "Distributed secondary frequency and voltage control of parallel-connected vscs in microgrids: A predictive vsg-based solution," *CPSS Trans. Power Electron. Appl.*, vol. 5, no. 4, pp. 342–351, 2020.

[3] H. A. Young, M. A. Perez, and J. Rodriguez, "Analysis of finite-control-set model predictive current control with model parameter mismatch in a three-phase inverter," *IEEE Trans. Ind. Electron.*, vol. 63, no. 5, pp. 3100–3107, 2016.

[4] Y. Yang, S. C. Tan, and S. Y. R. Hui, "Adaptive reference model predictive control with improved performance for voltage-source inverters," *IEEE Trans. Control Syst. Technol.*, vol. 26, no. 2, pp. 724–731, 2018.

[5] M. Easley, A. Y. Fard, F. Fateh, M. B. Shadmand, and H. Abu-Rub, "Auto-tuned model parameters in predictive control of power electronics converters," in *Proceedings of IEEE*, pp. 3703–3709, 2019.

[6] M. Khalilzadeh, S. Vaez-Zadeh, and M. S. Eslahi, "Parameter-free predictive control of ipm motor drives with direct selection of optimum inverter voltage vectors," *IEEE J. Emerg. Sel. Top. Power Electron.*, vol. 9, no. 1, pp. 327–334, 2021.

[7] M. A. Qureshi, F. Torelli, S. Musumeci, A. Reatti, A. Mazza, and G. Chicco, "A novel adaptive control approach for maximum power-point tracking in photovoltaic systems," *Energies*, vol. 16, no. 6, p. 2782, 2023.

[8] P. G. Carlet, F. Tinazzi, S. Bolognani, and M. Zigliotto, "An effective model-free predictive current control for

synchronous reluctance motor drives," *IEEE Trans. Ind. Appl.*, vol. 55, no. 4, pp. 3781–3790, 2019.

[9] Y. Zhang, J. Jin, and L. Huang, "Model-free predictive current control of pmsm drives based on extended state observer using ultralocal model," *IEEE Trans. Ind. Electron.*, vol. 68, no. 2, pp. 993–1003, 2021.

[10] J. Rodriguez, R. Heydari, Z. Rafiee, H. A. Young, F. Flores-Bahamonde, and M. Shahparasti, "Model-free predictive current control of a voltage source inverter," *IEEE Access*, vol. 8, pp. 211104–211114, 2020.

[11] "Renewables 2018 global status report." Available online: https://www.ren21.net/wpcontent/uploads/2019/08/Full-Report-2018.pdf (accessed on 20 November 2019).

[12] "Sunrise—sr-p660 260-285—solar panel datasheet—enf panel directory." Available online: https://www.enfsolar.com/pv/panel-datasheet/crystalline/30542 (accessed on 23 November 2019).

[13] K. Osmani, A. Haddad, M. Alkhedher, T. Lemenand, B. Castanier, and M. Ramadan, "A novel mppt-based lithium-ion battery solar charger for operation under fluctuating irradiance conditions," *Sustainability*, vol. 15, no. 12, p. 9839, 2023.

[14] K. G. J. Nigel and R. Rajeswari, "Ai-based performance optimization of mptt algorithms for photovoltaic systems," *Automatika*, vol. 64, no. 4, pp. 837–847, 2023.

[15] Z. Chen, J. Qiu, and M. Jin, "Adaptive finite-control-set model predictive current control for ipmsm drives with inductance variation," *IET Electr. Power Appl.*, vol. 11, no. 5, pp. 874–884, 2017.

[16] A. Bechouche, D. O. Abdeslam, H. Seddiki, and A. Rahoui, "Estimation of equivalent inductance and resistance for adaptive control of three-phase pwm rectifiers," in *Proceedings of IEEE*, pp. 1336–1341, 2016.

[17] M. Mehreganfar, M. H. Saeedinia, S. ADavari, C. Garcia, and J. Rodriguez, "Sensorless predictive control of afe rectifier with robust adaptive inductance estimation," *IEEE Trans. Ind. Inform.*, vol. 15, no. 6, pp. 3420–3431, 2019.

[18] C. Bordons, F. Garcia-Torres, and M. Ridao, *Model Predictive Control of Microgrids*, vol. 358. Springer: Berlin/Heidelberg, Germany, 2020.

[19] Y. Zhang, J. Jiao, and J. Liu, "Direct power control of pwm rectifiers with online inductance identification under unbalanced and distorted network conditions," *IEEE Transactions on Power Electronics*, vol. 34, no. 12, pp. 12524–12537, 2019.

[20] M. Abdelrahem, C. M. Hackl, and R. Kennel, "Finite set model predictive control with on-line parameter estimation for active front-end converters," *Electr. Eng.*, vol. 100, no. 3, pp. 1497–1507, 2018.

[21] L. Huang, J. Coulson, J. Lygeros, and F. Dörfler, "Data-enabled predictive control for grid-connected power converters," in *Proceedings of IEEE*, pp. 8130–8135, 2019.

[22] P. G. Carlet, A. Favato, S. Bolognani, and F. Dörfler, "Data-driven predictive current control for synchronous motor drives," in *Proceedings of IEEE*, pp. 5148–5154, 2020.

[23] H. Teiar, H. Chaoui, and P. Sicard, "Almost parameter-free sensorless control of pmsm," in *Proceedings of IEEE*, pp. 004667–004671, 2015.

[24] C. Roldán-Blay, G. Escrivá-Escrivá, C. Roldán-Porta, and C. Álvarez Bel, "An optimisation algorithm for distributed energy resources management in micro-scale energy hubs," *Energy*, vol. 132, pp. 126–135, 2017.

[25] N. T. Mbungu, R. Naidoo, and R. C. Bansal, "Optimisation of grid connected hybrid photovoltaic wind-battery system using model predictive control design," *IET Renew. Power Gener.*, vol. 11, no. 14, pp. 1760–1768, 2017.

[26] E. D. Santis, A. Rizzi, and A. Sadeghian, "Hierarchical genetic optimization of a fuzzy logic system for energy flows management in microgrids," *Appl. Soft Computing*, vol. 60, pp. 135–149, 2017.

[27] N. Chettibi, A. Mellit, G. Sulligoi, and A. M. Pavan, "Adaptive neural network—based control of a hybrid ac/dc microgrid," *IEEE Trans. Smart Grid*, vol. 9, no. 3, pp. 1667–1679, 2016.

[28] A. Elgammal and M. El-Naggar, "Energy management in smart grids for the integration of hybrid wind–pv–fc–battery renewable energy resources using multi-objective particle swarm optimisation (mopso)," *The Journal of Engineering*, vol. 11, pp. 806–1816, 2018.

[29] A. Hussain, V. H. Bui, and H. M. Kim, "A resilient and privacy-preserving energy management strategy for networked microgrids," *IEEE Trans. Smart Grid*, vol. 9, no. 3, pp. 2127–2139, 2018.

[30] M. Jafari, Z. Malekjamshidi, D. D.-C. Lu, and J. Zhu, "Development of a fuzzy-logic-based energy management system for a multiport multioperation mode residential smart microgrid," *IEEE Transactions on Power Electronics*, vol. 34, no. 4, pp. 3283–3301, 2018.